JOURNAL OF SOLID STATE CHEMISTRY 54, 1–9 (1984)

Neutron Diffraction Studies on Natural Heulandite and Partially Dehydrated Heulandite

T. W. HAMBLEY AND J. C. TAYLOR

CSIRO, Division of Energy Chemistry, Lucas Heights Research Laboratories, Private Mail Bag 7, Sutherland, NSW, 2232, Australia

Received November 7, 1983; in revised form February 15, 1984

The structure of heulandite from Coonabarabran, New South Wales, was refined using single crystal neutron diffraction data. The monoclinic crystals, space group $C2/m$, have cell parameters a = 17.77(2), b = 17.95(2), c = 7.435(7) Å, β = 116.46(5)°. Refinement using 1143 observed ($F > 4\sigma(F)$) reflections gave a final R of 0.064. The crystal was partially dehydrated and the data collection and refinement repeated. Cell parameters were then a = 17.71(2), b = 17.74(2), c = 7.439(6) Å, β = 116.74(3)°. Refinement on 1101 observed ($F > 4\sigma(F)$) reflections gave a final R of 0.078. Their structures establish the hydrogen bonding networks and reveal that on dehydration, there is a movement of cations and water molecules. The significance of these findings with respect to the thermal instability of heulandite is considered.

Introduction

Heulandite is a thermally unstable platy zeolite of ideal composition $(Ca, Na_2)Al_2Si_7O_{18} \cdot 6H_2O$. If it is heated to above 250°C or severely dehydrated, there is an irreversible collapse of the lattice and of the zeolitic channels leading to the heulandite B structure (*1, 2*). Consequently, heulandite is of little use as either a catalyst or a dehydrating agent since both of these uses involve high temperatures and dehydration.

Clinoptilolites differ chemically from heulandite, by having higher Si/Al ratios and high alkali/alkaline earth ratios (*3*), but have identical aluminosilicate frameworks (*4*). The clinoptilolite structure, however, is resistant to collapse at temperatures up to 750°C (*1*). Mumpton (*5*) suggested that the greater thermal stability of clinoptilolite was due to its higher silica content. Mason and Sand (*3*), however, postulated that the increased proportion of sodium and potassium to calcium in clinoptilolite was the origin of the increased stability. This latter view is supported by the observation of Shepard and Starkey (*6*), that substitution of the calcium in heulandite with potassium produced a zeolite with the heat-resistant properties of clinoptilolite. However, calcium-exchanged clinoptilolite does not lose its thermal stability (*5*), hence it must be concluded that both chemical differences play an interrelated role in determining the thermal stabilities of clinoptilolite and heulandite. It is evident that cation location, and consequently water location, plays a critical role in determining the thermal stabilities and two different mechanisms have been proposed (*4, 7*), to explain this role.

We have undertaken neutron single crystal studies on natural heulandite, to establish the hydrogen bonding network, and on

0022-4596/84 $3.00

partially dehydrated heulandite in the hope of elucidating some of the processes which occur on dehydration. Hydrogen locations from neutron single crystal refinements not only offer the obvious advantage of establishing the hydrogen bonding network but also enable a clear distinction between cation and water sites. A brief report of a neutron single crystal study of heulandite has appeared previously (*8*), but details and discussion were limited to the zeolite framework.

Experimental

Preparation and Analysis of Samples

The natural heulandite sample was from Coonabarabran, New South Wales. Electron microprobe analysis was used to determine the chemical composition and the results are given in Table I. The analytical results are similar to those obtained previously on samples from Switzerland (*9*) and Iran (*10*), and confirm that the sample can be assigned as heulandite.

A single crystal bounded by the forms {100}, {010}, {0, 0, 1}, and {101}, with dimensions 9.5 × 2.1 × 10.3 mm, was cleaved from a larger fragment. Prior to collection of the second data set the crystal was partially dehydrated by heating to 70°C under vacuum for 18 hr. Relatively mild dehydration conditions were employed to avoid the possibility of a collapse of the structure which occurs when more than about 40% of the water is removed (*11*). For data collection the dehydrated crystal was sealed under vacuum in a quartz tube.

TABLE I

CHEMICAL ANALYSIS (%) FOR NATURAL HEULANDITE

SiO_2	56.07
Al_2O_3	15.24
CaO	4.54
Na_2O	1.61
BaO	0.61
SrO	0.40
H_2O	(17.6)

TABLE II

CRYSTAL DATA AND UNIT CELL PARAMETERS

	Natural heulandite	Dehydrated heulandite
$Ba_{0.1},Ca_{2.2},Na_{1.4},Sr_{0.1},Al_{7.9},Si_{28.5},O_{72} \cdot 24.5\ H_2O$		13.4 H_2O
F.wt.	2749.7	2549.7
Space group	*C2/m*	*C2/m*
a (Å)	17.77(2)	17.71(2)
b (Å)	17.95(2)	17.74(2)
c (Å)	7.435(7)	7.439(6)
β (°)	116.46(5)	116.74(3)
U (Å^3)	2123	2087
d_c (g cm^{-3})	2.15	2.03
Z	1	1

Unit cell parameters for each case were obtained from a least-square fit to the setting parameters of 50 reflections (Table II).

Data Collection

Neutron diffraction data were collected on the "2TANB" four-circle diffractometer provided by the Australian Institute of Nuclear Science and Engineering (AINSE) at the Australian Atomic Energy Commission's materials testing reactor HIFAR, using neutrons of wavelength 1.234 Å. An w-2θ scan was employed with the scan width varying from 1.80° for $2\theta < 45°$ to 2.25° for $2\theta < 80°$. The reflections were scanned in steps of 0.005° with the step time dependent on the intensity of the incoming neutron beam. Backgrounds were measured at each extreme of the scan for half the scan time. A hemisphere of reflections for $2\theta < 85°$ was collected for both data sets. A standard was monitored after the collection of every 20 reflections and any variation in intensity was corrected. All data were corrected for absorption and the Lorentz factor, analyzed, then merged using local data reduction programs to give 1440 and 1312 independent reflections for the natural and dehydrated crystal data sets, respectively.

Refinement of the Structures

The space group $C2/m$ was chosen on the basis of previous refinements of natural heulandite (*9*, *10*). The lower symmetry space group $C\,m$ was also possible; however, deviations from $C2/m$ were only slight, making a successful refinement in $C\,m$ difficult.

(*i*) *Natural heulandite.* Starting coordinates were taken from the final refinement of X-ray single crystal data (*10*). Occupancies of the water and cation sites were refined during the isotropic phase of refinement and generally were little different to those obtained by X-ray analysis (*10*). One water site [O(12)] was better modeled as two separate sites [O(12) and O(12′)] about 0.8 Å apart. Hydrogen atoms were located from difference Fourier maps and successfully refined. Only one hydrogen atom of O(16′) was located, but, this may have been due to overlap of the second site with the hydrogen atom of O(16). The hydrogen atoms of O(13) are disordered (60 : 40) over two sites. All atoms, except O(12), O(12′), O(15), O(16′), and their associated hydrogen atoms, were refined anisotropically.

Full-matrix least-square refinement of a scale factor and all positional and thermal parameters gave a final $R = \Sigma(||F_o| - |F_c||)/\Sigma|F_o| = 0.064$ on 1143 F with $I > 2\sigma(I)$. Final positional parameters are listed in Table III.

(*ii*) *Partially dehydrated heulandite.* Starting coordinates for the framework atoms were taken from the refinement of the natural heulandite. Water molecules and cations were located from difference Fourier maps and their occupancies were refined. Hydrogen atoms of all water molecules were located and successfully refined. Most water molecules showed some depletion in occupancy when compared with natural heulandite and one new water site appeared. Likewise, the cation sites were depleted and a new cation site was occupied. Due to the reduced occupancies only O(11), H(1), O(12), H(2), O(13), O(14), CS(1), and CS(2) could be refined anisotropically.

Full-matrix least-square refinement, as before, converged with $R = 0.078$ on 1101 F with $I > 2\sigma(I)$. Final positional parameters are given in Table IV.

TABLE III

NATURAL HEULANDITE: POSITIONAL PARAMETERS ($\times 10^4$)

	x	y	z	Occupancy
Si(1)	1791(3)	1696(2)	950(5)	1.0
Si(2)	2114(3)	4098(2)	5002(5)	1.0
Si(3)	2086(3)	1911(2)	7169(5)	1.0
Si(4)	650(2)	2991(2)	4117(5)	1.0
Si(5)	0	2129(3)	0	1.0
O(1)	1968(3)	½	4551(7)	1.0
O(2)	2315(2)	1202(2)	6126(5)	1.0
O(3)	1828(2)	1544(2)	8835(5)	1.0
O(4)	2382(2)	1067(2)	2539(4)	1.0
O(5)	0	3254(3)	½	1.0
O(6)	821(2)	1591(2)	615(5)	1.0
O(7)	1282(2)	2347(2)	5506(5)	1.0
O(8)	98(2)	2669(2)	1858(5)	1.0
O(9)	2102(2)	2542(2)	1761(5)	1.0
O(10)	1154(2)	3734(2)	4000(5)	1.0
O(11)	2214(5)	½	−174(12)	1.0
H(1)	2312(8)	4627(7)	−925(28)	1.0
O(12)	786(28)	0	8901(48)	0.6
H(2)	799(30)	425(41)	9327(80)	0.6
O(12′)	955(58)	0	8091(98)	0.4
H(2′)	341(50)	0	8180(98)	0.4
H(2″)	1234(77)	0	8163(90)	0.4
O(13)	758(6)	4179(6)	9678(28)	0.9
H(3)	826(40)	3857(41)	9808(93)	0.4
H(4)	861(25)	3985(33)	949(52)	0.4
H(3′)	646(20)	3612(27)	9329(59)	0.5
H(4′)	1307(12)	4421(11)	9702(23)	0.5
O(14)	0	½	½	1.0
H(5)	0	4548(14)	½	1.0
O(15)	285(10)	951(26)	4970(38)	0.3
H(6)	344(20)	1369(37)	5004(58)	0.3
H(7)	96(89)	921(70)	6250(94)	0.3
O(16)	984(10)	0	2798(23)	0.72
H(8)	991(14)	471(27)	2342(42)	0.72
O(16′)	805(30)	385(38)	3766(78)	0.14
H(8′)	297(72)	0	2939(97)	0.28
CS(1)	1567(9)	0	6701(27)	0.6
CS(2)	418(8)	½	2069(22)	0.52

Scattering amplitudes were taken from Bacon (*12*). Silicon amplitudes were used for all silica/aluminum sites except Si(2) where an amplitude corresponding to 60% silicon and 40% aluminum was used. For cation site (2) the calcium scattering amplitude was employed, whereas for cation site (1) an amplitude midway between calcium and sodium was used.

Structure factor tables, bond lengths, and angles for the water molecules and tables of anisotropic thermal parameters for both refinements have been deposited.[1]

Discussion

(*i*) *Natural Heulandite*

Refinement of the heulandite structure using neutron diffraction data gives positional coordinates and occupancies, for both framework and occluded atoms, which are very similar to those obtained from X-ray analysis (*10*).

The secondary building unit (sbu) of heulandite can be described as either a "4-4-1" (*13*) or a $T_{10}O_{20}$ unit (*14*). In fact, these units share silicon atoms, so though the 4-4-1 description is more accurate, $T_{10}O_{20}$ better describes the resultant structural unit. In the heulandite structure the sbu's link to form sheets which lie parallel to the *ac* plane at $y = 0$ and $y = 1/2$. There are relatively few links between these sheets and this gives rise to the microporous structure and the facile cleavage parallel to the *ac* plane.

[1] See NAPS document No. 04187 for 17 pages of supplementary material. Order from ASIS/NAPS, Microfiche Publications, P.O. Box 3513, Grand Central Station, New York, NY 10163. Remit in advance $4.00 for microfiche copy or for photocopy, $7.75 up to 20 pages plus $.30 for each additional page. All orders must be prepaid. Institutions and organizations may order by purchase order. However, there is a billing and handling charge for this service of $15. Foreign orders add $4.50 for postage and handling, for the first 20 pages, and $1.00 for additional 10 pages of material. Remit $1.50 for postage of any microfiche orders.

TABLE IV

DEHYDRATED HEULANDITE: POSITIONAL PARAMETERS ($\times 10^4$)

	x	*y*	*z*	Occupancy
Si(1)	1791(3)	1670(3)	929(6)	1.0
Si(2)	2087(3)	4092(3)	4974(7)	1.0
Si(3)	2108(3)	1897(3)	7219(6)	1.0
Si(4)	647(3)	2955(3)	4111(6)	1.0
Si(5)	0	2083(4)	0	1.0
O(1)	1926(5)	½	4501(9)	1.0
O(2)	2355(3)	1196(3)	6178(6)	1.0
O(3)	1836(3)	1492(2)	8812(5)	1.0
O(4)	2415(3)	1072(2)	2568(5)	1.0
O(5)	0	3222(4)	½	1.0
O(6)	822(2)	1548(2)	601(6)	1.0
O(7)	1325(3)	2345(3)	5523(6)	1.0
O(8)	104(3)	2621(3)	1875(6)	1.0
O(9)	2083(2)	2548(2)	1614(5)	1.0
O(10)	1114(3)	3731(2)	3948(6)	1.0
O(11)	2124(10)	½	−321(21)	0.6
H(1)	2185(27)	4569(10)	−1137(37)	0.6
O(12)	746(20)	0	8836(56)	0.5
H(2)	664(22)	404(21)	9268(71)	0.5
O(13)	732(10)	4178(10)	9676(23)	0.5
H(3)	808(46)	3643(48)	9458(72)	0.3
H(4)	749(32)	4049(30)	973(83)	0.3
H(3′)	436(54)	3623(57)	9550(92)	0.2
H(4′)	1313(50)	4413(44)	9821(98)	0.2
O(13″)	718(58)	½	9875(98)	0.2
H(3″)	1018(70)	½	9163(99)	0.2
H(4″)	1063(70)	½	10604(90)	0.2
O(14)	0	½	½	1.0
H(5)	0	4382(43)	½	0.35
H(5′)	4559(32)	328(24)	5180(60)	0.35
O(16)	943(23)	0	3003(66)	0.3
H(8)	957(31)	462(32)	2311(71)	0.3
O(16′)	780(52)	363(50)	4001(90)	0.12
H(8′)	275(62)	0	3258(92)	0.24
H(9′)	788(89)	790(80)	3250(95)	0.12
CS(1)	1744(20)	0	7052(35)	0.44
CS(2)	351(10)	½	2411(21)	0.45
CS(3)	½	4133(40)	½	0.24

The major channel systems lie in the *ac* plane, parallel to *c*, and at about 50° to *a*. Minor channels also run roughly perpendicular to both systems. In Fig. 1 atoms plotted as van de Waals radius spheres give a true indication of the void area of these channels. There are two channels which lie parallel to *c*, a large elliptical one centered at $x = 0$, $y = 0$, and a smaller more circular channel at $x = 1/2$, $y = 0$. The void dimensions of these channels are about 7.5 × 3.0 and 4.3 × 3.3 Å. The channels lying at 50° to *a* are more circular but smaller, having dimensions of about 3.1 × 3.3 Å. They also

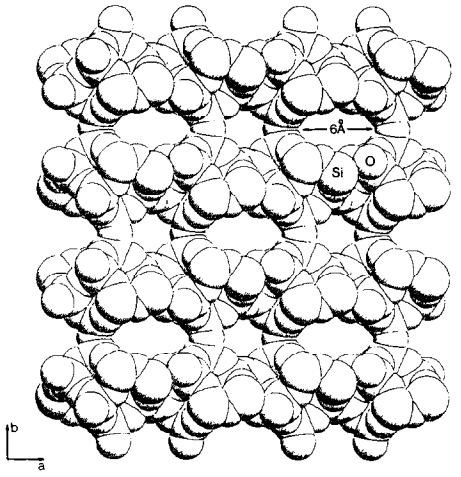

FIG. 1. A view parallel to c of natural heulandite, with the atoms drawn as van de Waal's radius spheres, showing the size of the channels.

lie at $y = 0$. Cation site (1) lies in the larger elliptical channel and cation site (2) in the smaller channel. An ORTEP plot of the bonding and hydrogen bonding of the cation–water systems in the channels is shown in Fig. 2.

Cation (1), which is believed to be about 50% sodium and 50% calcium (*10*), is bonded to framework oxygen O(2) twice, to water oxygen O(15) twice, and to water oxygens O(11), O(12), and O(16), making it seven-coordinate. Full occupancy of cation site (1) is evidently precluded by the clash (about 1 Å) of O(15) atoms of adjacent $(1 - x, 1 - y, 1 - z)$ units. The occupancy of CS(1) refined to 60%, however, greater than half occupancy is possible since the occupancy of O(15) is only 30%. When CS(1) is vacant, O(12) apparently moves to site O(12′) (these were previously refined as a single atom (*10*)) and O(16) moves to O(16′). Oxygen site O(11) is fully occupied and is presumably held in place by the moderately strong hydrogen bonds to the framework when CS(1) is vacant. Hydrogen atoms of O(12), O(15), and O(16) are also involved in possible hydrogen bonds with framework oxygens.

Cation site (2) is believed to be occupied by calcium only (*10*). It is bonded to three framework oxygens, O(10) twice and O(1), to water oxygen O(14) and to water oxygen O(13) four times (at two different distances). Again CS(2) cannot be fully occupied because of a clash with an adjacent

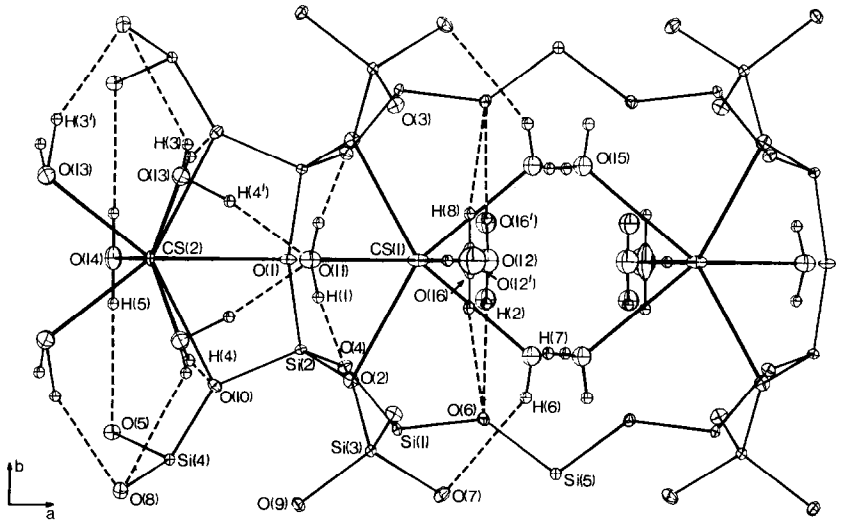

FIG. 2. An ORTEP plot, parallel to c, showing the cation and hydrogen bonding networks in natural heulandite.

$(-x, 1 - y, -z)$ unit; however, here the exclusion is strict because the CS(2) . . . CS(2)′ separation is only 2.75 (3) Å. The occupancy of CS(2) refined to 50% indicating that the smaller channel is fully occupied. Also, the associated water molecules are present at the 100% level; O(14) is equidistant from adjacent CS(2) sites and the O(13) atoms which are bonded at longer distances to CS(2) are bonded at shorter distances to CS(2)′ and vice versa. The hydrogen atoms of O(14) apparently have hydrogen bonds with the framework oxygen O(5). The hydrogens of O(13) are disordered over two sites, presumably as a consequence of the disorder of CS(2). They also apparently have hydrogen bonds with framework oxygens and water oxygen O(11). Oxygen to cation bonding distances for both sites are listed in Table V while distances which correspond to possible hydrogen bonds are given in Table VI.

Average silicon to oxygen bond lengths for each silicon site are listed in Table VII for natural and dehydrated heulandite. The distances are almost identical to those observed in the X-ray single crystal study (*10*), the bond lengths to Si(2) being significantly longer than all others. If it is assumed that the extension of the bonds to Si(2) is due to occupation of the site by aluminum then a Si/Al ratio of about 1 is calculated (*15*). All other sites are apparently occupied by 10–20% aluminum. The presence of more aluminum at site Si(2) is significant, as three oxygens bonded to it are also bonded to cations and the fourth is hydrogen bonded to a water molecule. Olson (*16*), discussing the structure of zeolite NaX, suggested that the location of occluded cations and framework aluminum is correlated, primarily as a result of the greater electronegativity of aluminum compared with silicon. Thus, it is probable that here, the presence of relatively more aluminum at site Si(2) is related to the location and bonding of the cations.

TABLE V

CATION–OXYGEN BOND LENGTHS (Å)

Bond	Natural heulandite	Dehydrated heulandite
CS(1)–O(2)	2.65(1)	2.59(2)
CS(1)–O(2)[a]	2.65(1)	2.59(2)
CS(1)–O(11)[b]	2.51(1)	2.36(3)
CS(1)–O(12)	2.57(3)	2.65(5)
CS(1)–O(15)	2.65(3)	—
CS(1)–O(15)[a]	2.65(3)	—
CS(1)–O(16)	2.61(4)	2.69(5)
CS(1)–O(3)	—	2.92(2)
CS(1)–O(3)[a]	—	2.92(2)
CS(2)–O(1)	2.53(1)	2.51(2)
CS(2)–O(10)	2.67(1)	2.61(1)
CS(2)–O(10)[a]	2.67(1)	2.61(1)
CS(2)–O(13)	2.57(2)	2.82(3)
CS(2)–O(13)[b]	2.39(2)	2.35(3)
CS(2)–O(13)[a]	2.57(2)	2.82(3)
CS(2)–O(13)[c]	2.39(2)	2.35(3)
CS(2)–O(14)	2.60(2)	2.27(2)
CS(2)–O(13′)	—	2.25(8)
CS(3)–O(12)	—	2.98(5)
CS(3)–O(12)[b]	—	2.98(5)
CS(3)–O(16′)	—	2.85(7)
CS(3)–O(16′)[c]	—	2.85(7)

[a] $x, -y, z$.
[b] $-x, -y, -z$.
[c] $-x, y, -z$.

(*ii*) *Partially Dehydrated Heulandite*

Partial dehydration of heulandite, under the conditions described above, leads to significant changes in the lattice constants (Table II). The largest variations are in the reduction of b and the increase in β, though a slight decrease in a is also evident. These changes are consistent with a partial collapse of the structure toward heulandite B, the heat collapsed phase.

Refinement of the occupancies of the water sites in dehydrated heulandite shows that most sites are depleted and gives a total water content of 13.4 molecules per unit cell compared with 23.6 in natural heulandite. Studies of the dehydration properties of heulandite show that it loses c 50% of its

TABLE VI

CLOSE CONTACTS (Å) CORRESPONDING TO POSSIBLE HYDROGEN BONDS

Atoms	Natural heulandite		Dehydrated heulandite	
	O . . . O	O . . . H	O . . . O	O . . . H
O(11)–H(1) . . . O(4)[a]	2.88	1.96	2.88	1.90
O(14)–H(5) . . . O(5)	3.10	2.30	3.15	2.06
O(12)–H(2) . . . O(6)[b]	3.09	2.27	3.02	2.22
O(16)–H(8) . . . O(6)	3.20	2.31	3.23	2.26
O(15)–H(6) . . . O(7)	2.96	2.31	—	—
O(13)–H(3) . . . O(8)[c]	3.04	2.61	3.10	2.33
O(13)–H(3′) . . . O(8)[c]	3.04	2.07	3.10	2.07
O(13)–H(4) . . . O(10)[b]	3.07	2.14	3.14	2.08
O(13)–H(4′) . . . O(11)[b]	2.92	1.88	2.86	1.82
O(12′)–H(2″) . . . O(11)[d]	2.90	2.48	—	—
O(16′)–H(8′) . . . O(15)[e]	2.83	2.27	—	—

[a] $1/2 - x, 1/2 - y, -z$.
[b] $x, y, z + 1$.
[c] $-x, y, 1 - z$.
[d] $1/2 - x, 1/2 - y, 1 - z$.
[e] $x, -y, z$.

water content easily and any further water loss results in collapse of the zeolitic cavities (*1*). Thus, it appears that we have removed nearly all the loosely bound water.

The two water sites removed completely on partial dehydration are O(12′), which in natural heulandite, is not bonded to a cation, and O(15) which is bonded to CS(1). Of the other sites O(11), O(16), and O(16′) move from 0.1 to 0.3 Å in the z direction. The hydrogen bonding and cation bonding networks of natural heulandite are essentially retained (Fig. 3). A new water site, designated O(13′), lies 2.25(8) Å from CS(2).

TABLE VII

MEAN Si–O BOND LENGTHS (Å)

Natural heulandite		Dehydrated heulandite	%Al
Si(1)	1.624(6)	1.636(13)	14
Si(2)	1.652(15)	1.656(9)	32
Si(3)	1.619(13)	1.623(13)	7
Si(4)	1.618(10)	1.621(15)	7
Si(5)	1.625(5)	1.627(9)	11

Both cation sites (1) and (2) move significantly in the x and z directions and refinement of their occupancies suggested that each is depleted – CS(1) by ca. 20% and CS(2) by ca. 10%. A new site [CS(3)] appears near the center of the unit cell, and larger channel, and its refined occupancy is consistent with the depletion of sites CS(1) and CS(2). Although it is possible that CS(3) is in fact a water molecule all attempts to locate sensible hydrogen atom sites in the difference maps were unsuccessful. CS(3) is loosely bonded to water and framework oxygens.

Cation to oxygen distances are listed in Table V and distances corresponding to possible hydrogen bonds are given in Table VI.

(*iii*) *The Influence of the Cations and Water Molecules on the Thermal Stability of Heulandite*

This structural analysis of partially dehydrated heulandite establishes the partial depletion of all water sites, except O(14), and

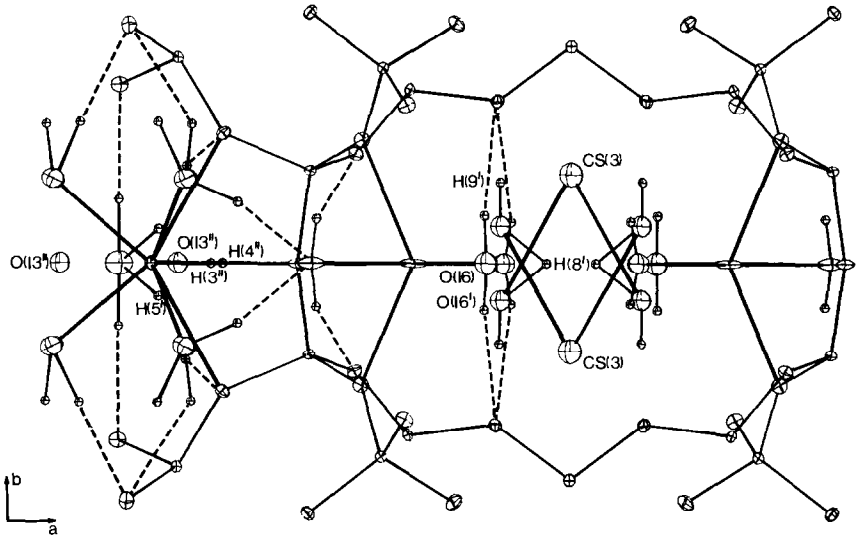

FIG. 3. An ORTEP plot, parallel to *c*, showing the cation and hydrogen bonding networks in partially dehydrated heulandite.

both cation sites, and the appearance of a new cation site. These results are consistent with a partial transformation to heulandite B in which only water site O(14) is occupied and all cations have moved from CS(1) and CS(2). We now address the question of whether these observations can explain the collapse of natural heulandite on dehydration or heating, and, further, whether they give any insight into the greater stability of heulandite's related zeolite, clinoptilolite.

Both cation sites in natural heulandite are bonded to framework oxygens and depletion of these sites could reasonably be expected to lead to collapse of the framework. Thus, it appears that removal of the water from heulandite destabilizes the cation sites, which subsequently move and cause the structure to collapse. This sequence of events is supported by the observation of a new cation site in partially dehydrated heulandite and the vacancy of CS(1) and CS(2) in heulandite B(*2*).

In clinoptilolite, much of the Ca present in heulandite is replaced by monovalent cations (Na and K) and consequently there are more cations per unit cell. As a result, additional cation sites are observed in the clinoptilolite structure (*4*, *7*). In all structures of clinoptilolites a cation site has been observed at the origin of the cell (*4*, *7*), a position not occupied in natural heulandite. In partially dehydrated heulandite, the new cation site [C(3)] lies only 1.5 Å from the origin of the cell. It is probable that in clinoptilolite the occupancy of additional sites, and in particular the site at the cell origin, precludes the movement of the cations from their framework bonded positions [CS(1) and CS(2)] and so enhances the stability of the structure.

Koyama and Takeuchi (*7*) located an additional cation site in clinoptilolite at a position only about 0.6 Å from the site occupied by water O(11) in the heulandite structure. They suggested that the presence of this cation, weakly bonded to the framework, supported the framework and stabilized the clinoptilolite structure (*7*). Considering the weakness of the bonds between this "cation" and the framework, this conclusion is

somewhat surprising. The shortest interaction between this cation site and the framework is about 3.0 Å and any collapse of the structure would result in shorter and stronger bonds and thus be promoted by the cation. Also, the proximity of this "cation" site to water oxygen O(11) leads us to suggest that it may be a water oxygen site, occupied by O(11) when the adjacent cation site [CS(1)] is vacant.

Alberti (*4*) suggested that the presence of a cation at CS(1) was critical in stabilizing the zeolitic structure, lying as it does, at the crossing of channel systems; our results are consistent with this assumption.

Acknowledgments

We thank Dr. L. Sutherland and Mr. R. Pogson, of the Australian Museum, Sydney, for donating the crystal of heulandite, Dr. F. H. Moore of AINSE for use of neutron diffraction facilities, Ms. S. A. Miller for assistance with the computing, and the Electron Microscope Unit, University of Sydney, for the elemental analysis. T. W. H. acknowledges the Australian Institute of Nuclear Science and Engineering for the award of a Postdoctoral Fellowship.

References

1. A. Alietti, *Amer. Mineral.* **57,** 28 (1972).
2. A. Alberti, *Tschermaks Mineral. Petrogr. Mitt.* **19,** 173 (1973).
3. B. Mason and L. B. Sand, *Amer. Mineral.* **45,** 341 (1960).
4. A. Alberti, *Tschermaks Mineral. Petrogr. Mitt.* **22,** 25 (1975).
5. F. A. Mumpton, *Amer. Mineral.* **45,** 351 (1960).
6. A. O. Shepard and H. C. Starkey, *U.S. Geol. Surv. Prof. Pap.* **475D,** 89 (1964).
7. K. Koyama and Y. Takeuchi, *Z. Kristallogr.* **145,** 216 (1977).
8. H. Bartl, *Z. Kristallogr.* **137,** 440 (1973).
9. A. B. Merkle and M. Slaughter, *Amer. Mineral.* **53,** 1120 (1968).
10. N. Bresconi-Pahor, M. Calligoris, G. Nordin, L. Randaccio, E. Russo, and P. Comin-Chiaramonti, *J. Chem. Soc., Dalton Trans.* 1511 (1980).
11. M. H. Simonot-Grange and A. Cointot, *Bull. Soc. Chim. Fr.* **2,** 421 (1969).
12. G. E. Bacon, *in* "Neutron Diffraction Newsletter" (W. B. Yelon, Ed.), Oxford Univ. Press, London/New York 1977.
13. R. Gramlich-Meier and W. M. Meier, *J. Solid State Chem.* **44,** 41 (1982).
14. W. J. Mortier and J. R. Pearce, *Amer. Mineral.* **66,** 309 (1981).
15. J. V. Smith and S. W. Bailey, *Acta Crystallogr.* **16,** 801 (1963).
16. D. H. Olson, *J. Phys. Chem.* **74,** 2758 (1970).